Intrinsic anharmonic effects on the phonon frequencies and effective spin-spin interactions in a quantum simulator made from trapped ions in a linear Paul trap

M. McAneny and J. K. Freericks[*]

Department of Physics, Georgetown University, 37th and O Streets NW, Washington, DC 20057, USA
(Received 20 June 2014; published 6 November 2014)

The Coulomb repulsion between ions in a linear Paul trap gives rise to anharmonic terms in the potential energy when expanded about the equilibrium positions. We examine the effect of these anharmonic terms on the accuracy of a quantum simulator made from trapped ions. To be concrete, we consider a linear chain of Yb^{171+} ions stabilized close to the zigzag transition. We find that for typical experimental temperatures, frequencies change by no more than a factor of 0.01% due to the anharmonic couplings. Furthermore, shifts in the effective spin-spin interactions (driven by a spin-dependent optical dipole force) are also, in general, less than 0.01% for detunings to the blue of the transverse center-of-mass frequency. However, detuning the spin interactions near other frequencies can lead to non-negligible anharmonic contributions to the effective spin-spin interactions. We also examine an odd behavior exhibited by the harmonic spin-spin interactions for a range of intermediate detunings, where nearest-neighbor spins with a larger spatial separation on the ion chain interact more strongly than nearest neighbors with a smaller spatial separation.

I. INTRODUCTION

In 1982, Richard Feynman opened the field of quantum simulation when he proposed that quantum simulators can be employed in order to study the evolution and interactions of complex quantum mechanical systems [1]. It is only recently that ion trap quantum simulators have demonstrated success in engineering model spin-systems in both one-dimensional and two-dimensional lattices of trapped ions [2–13]. Starting with the demonstration of the effective spin interaction between two ions [2], it was shown that larger numbers of ions interact with well-defined Ising spin exchange [3], which can show frustration [4,5], and can be scaled to approximate the thermodynamic phase transition [6]. Penning trap experiments [7,8], showed that the same concepts can be extended to hundreds of ions trapped in a rotating triangular lattice. The idea of stroboscopic quantum simulation has also been shown [9]. Recently, Paul trap systems have been scaled up to 18 ions [10] and properties of dynamics and excited states have been examined via Lieb-Robinson-like studies of correlation growth [11,12] and spectroscopy of excited states [13]. These ion-trap systems work well due to their long decoherence times, scalability, and ability to be precisely controlled experimentally.

As the precision of these experiments grows, one needs to examine perturbations of these systems that carry them away from the simplest ideal. In addition, as the system sizes grow, it becomes increasingly difficult to fully cool the systems down to low temperatures as Raman sideband cooling becomes more complex and difficult to carry out. Hence, it is often only the phonon modes that are to be driven that are cooled below the Doppler limit; the phonons in other spatial directions are often left at the Doppler limit, which can have them with tens to hundreds of quanta excited.

Anharmonic effects enter into an oscillator when the period of the oscillation depends on its amplitude. In solid state physics, anharmonic effects are well known in causing lattices to (typically) expand as they are heated. Another way of describing this behavior is that as anharmonic terms are considered, they break the simple picture of free normal modes that oscillate at their own independent frequencies into a coupled oscillator system that can have its periods change, that can have resonantly enhanced dissipations, and that can excite quanta in the coupled modes. It is impossible to completely remove anharmonic effects from an ion trap, even if the trapping potentials can be made purely harmonic, because there is an intrinsic anharmonicity that arises due to the Coulomb interaction between the ions. In this work, we investigate whether such anharmonic effects are likely to cause inaccuracies in a quantum simulation. We should emphasize that we are not examining any other effects that might modify the operation of these simulators. Our goal is to determine at what level intrinsic anharmonic effects enter and whether they are small enough to be neglected in the analysis of the quantum simulator.

Anharmonic effects have been considered previously for linear Paul traps. Marquet *et al.* showed how one can determine the coupling tensors that arise due to the anharmonic nature of the Coulomb interaction and how one can use those couplings to resonantly dissipate energy from one mode to the other modes via optical-mixing-like effects [14]. This transfer of energy from one mode to another was investigated experimentally in a two-site chain [15]. The effects of anharmonicities in either the potentials or the Coulomb interaction were investigated to see how phonon frequencies shift due to the occupancy of other phonon modes [16]. Anharmonic quantum effects on the zigzag transition were investigated with a renormalization-group approach based on path integrals [17]. In this work, we focus on how the intrinsic anharmonicity affects the phonon frequencies and how these, in turn, affect the Ising spin exchange couplings. Hence, we do not treat anharmonic effects in the trapping potential, but only those that arise from the Coulomb interaction.

The remainder of this paper is organized as follows: In Sec. II, we discuss the formalism for determining anharmonic

---

[*]freericks@physics.georgetown.edu

effects, numerical results follow in Sec. III, and we conclude in Sec. IV. Details of the anharmonic coupling tensors appear in the Appendixes.

II. THEORETICAL FORMULATION

We consider a chain of ions in a linear Paul trap, which uses a combination of static and time-dependent fields in order to trap ions. The precise behavior of this system often includes micromotion due to the time-dependent fields, but it is well described by a static pseudopotential when the ion equilibrium positions lie at the nulls of their potential energy surface. We provide our analysis under the assumption that the static pseudopotential approach is accurate for describing the motion of the ions in the trap.

The potential energy describing such a system of N ions includes both a term describing the Coulomb interaction between each pair of ions and a term related to the spring energy of each ion along the z axis (which will be the axis of longitudinal alignment for the ions). The dimensionless potential is then given by

$$V = \frac{1}{2} \sum_{\alpha=x,y,z} \sum_{i=1}^{N} \beta_\alpha^2 x_{i\alpha}^2 + \frac{1}{2} \sum_{\substack{i,j=1 \\ i \neq j}}^{N} \frac{1}{|\mathbf{r}_i - \mathbf{r}_j|}, \quad (1)$$

where the potential has been scaled by $m\omega_z^2 l_0^2$, and the dimensionless ion coordinates $\mathbf{r}_i = (x_{ix}, x_{iy}, x_{iz})$ have been renormalized by a characteristic length $l_0 = [kZ^2e^2/(m\omega_z^2)]^{1/3}$, with k the Coulomb coupling constant, Z the charge on the ion, e the charge of an electron, and m the mass of the ion. In addition, we have $\beta_\alpha = \omega_\alpha/\omega_z$, where ω_α is the trapping frequency in the αth direction. We consider the case with $\beta_x = \beta_y \gg \beta_z = 1$, which gives rise to a one-dimensional chain for the ions, if the number of ions N lies below a critical value. The choice $\beta_x = \beta_y$ is for convenience only, as experimental systems usually change these to be different from one another by a few percent. The degeneracies that arise from setting them equal do not affect our general results, and allow us to use one fewer parameter in the numerical calculations.

From Eq. (1), the equilibrium positions are readily found numerically by using nonlinear optimization routines to find where the potential has a minimum and the force vanishes [14]. Then, by expanding the potential to fourth order in the coordinates of the ions about their equilibrium positions, one obtains the Hamiltonian written in the phonon creation and annihilation operator basis as follows:

$$\mathcal{H} = \sum_{\nu=1}^{3N} \varepsilon_\nu \left(\hat{a}_\nu^\dagger \hat{a}_\nu + \frac{1}{2} \right)$$

$$+ \sum_{\nu,\nu',\nu''=1}^{3N} B_{\nu,\nu',\nu''} (\hat{a}_\nu + \hat{a}_\nu^\dagger)(\hat{a}_{\nu'} + \hat{a}_{\nu'}^\dagger)(\hat{a}_{\nu''} + \hat{a}_{\nu''}^\dagger)$$

$$+ \sum_{\nu,\nu',\nu'',\nu'''=1}^{3N} C_{\nu,\nu',\nu'',\nu'''} (\hat{a}_\nu + \hat{a}_\nu^\dagger)(\hat{a}_{\nu'} + \hat{a}_{\nu'}^\dagger)$$

$$\times (\hat{a}_{\nu''} + \hat{a}_{\nu''}^\dagger)(\hat{a}_{\nu'''} + \hat{a}_{\nu'''}^\dagger), \quad (2)$$

where the scaled normal-mode (phonon) energies satisfy $\varepsilon_\nu = \hbar\omega_\nu/(m\omega_z^2 l_0^2)$, and the explicit values for the cubic and quartic coupling tensors B and C are given in the Appendixes. The ν subscript denotes the specific normal mode, which is indexed from 1 to $3N$.

At this stage, it is appropriate to treat these higher order terms as a perturbation to the harmonic Hamiltonian because they should correspond to small corrections to the potential when the ions remain close to their equilibrium positions. The third-order term creates no first-order shift to the energy spectrum, as it contains an odd number of creation and annihilation operators. Therefore, a second-order perturbation expansion is required for that term. The quartic term gives rise to a first-order shift in perturbation theory and hence that term is also included. Then, using time-independent Rayleigh-Schrödinger perturbation theory, the anharmonic shifts can be calculated to first order in C and second order in B, as has been done in previous work [16]. This approach will calculate the changes to fourth order in the expansion of the frequencies and even include some of the sixth-order corrections. To get the remaining sixth-order corrections would require us to expand the Coulomb interaction two more orders to determine the sixth-order coupling tensor and evaluate its shift on the energy levels to first order in perturbation theory. That calculation and all other higher order corrections are beyond the scope of this work. While we cannot rigorously show that this approach determines all of the anharmonic effects, it should be able to accurately calculate anharmonic effects for the smallest deviations from the harmonic model.

Before proceeding, it is relevant to note that the anharmonic frequency shifts of the center-of-mass modes (both transverse and longitudinal) can be found to identically vanish through fourth order. This was shown explicitly to third order [14] and can be immediately generalized to all orders, because the center-of-mass mode decouples from anharmonic corrections when the trap potential is purely harmonic (as we have chosen here, since we assume that the pseudopotential that describes the trap has no anharmonic terms) and the inter-ion forces satisfy Newton's third law [18,19] (as they do for the Coulomb interaction). Hence the center-of-mass frequency is fixed at the corresponding trap frequency.

In general, the shifts in frequency (scaled by the transverse center-of-mass frequency, $\omega_{\text{c.m.}}$) can then be written as a function of the occupation number of each mode as

$$\frac{\Delta\omega_\nu(n_\nu, \{n_{\nu'}\})}{\omega_{\text{c.m.}}} = \frac{\Delta E(n_\nu + 1, \{n_{\nu'}\}) - \Delta E(n_\nu, \{n_{\nu'}\})}{\varepsilon_{\text{c.m.}}}, \quad (3)$$

where c.m. denotes the center of mass, and $\{n_{\nu'}\}$ is the set of occupation numbers for all $\nu' \neq \nu$. This is an intuitive definition for the anharmonic frequency shifts, since it is the relative energy shift caused by adding one more phonon to the system with harmonic frequency ω_ν (when there are already n_ν phonons in that mode and the other modes are occupied according to $\{n_{\nu'}\}$) [16]. The ΔE terms are the shifts in the anharmonic energies from the harmonic result and, hence, vanish when there is no anharmonicity. Their explicit form is given in Appendix C.

The ions in the trap often have an internal hyperfine structure which can be mapped onto Ising spin variables. For the Yb^{171+} ion, one usually takes the clock states as the

"spin-up" and "spin-down" states. This internal (spin) degree of freedom can be coupled to the motional degrees of freedom by applying a spin-dependent optical dipole force. This is usually done by applying red and blue detuned laser beams ($\omega \pm \mu$) on top of a carrier beam at ω. By considering the ac Stark effect caused by these beams and factorizing the resulting evolution operator, one can realize a spin-dependent optical dipole force on the ions [20,21]. In this way, the motional degrees of freedom of the system are coupled to the spin degrees of freedom, generating the following Ising Hamiltonian when one has harmonic phonons:

$$\mathcal{H}_{\text{Ising}} = \sum_{i,j} J_{i,j}(t) \sigma_i^x \sigma_j^x, \tag{4}$$

with exchange coefficients that depend on time. The time-independent piece of the spin-spin couplings is [21]

$$J_{i,j} = \frac{F_O^2}{4m} \sum_{\nu=1}^{N} \frac{b_i^{x\nu} b_j^{x\nu}}{\mu^2 - \omega_\nu^2}, \tag{5}$$

where F_O is the magnitude of the spin-dependent optical dipole force and $b_i^{\alpha\nu}$ is the αth spatial component of the ith ion's transverse phonon eigenvector corresponding to the ω_ν mode. In this summation, we only take the modes that lie in the direction of the driving force, which is typically the (transverse) $\alpha = x$ direction.

It is difficult to extend this derivation to include the cubic and quartic phonon-mode coupling terms in the phonon Hamiltonian, because the operator factorization of the evolution operator becomes much more complicated (see, for example, Ref. [22], which shows how to factorize the evolution operator and describes the problems that arise from noncommuting operators). Therefore, rather than calculating these complicated terms, it is assumed that these terms are small because the ions do not deviate far from their equilibrium positions. The factorization of the laser-ion evolution operator begins with rewriting the evolution operator in the interaction representation with respect to the phonon Hamiltonian (which is time independent). The full evolution operator is just a product of the evolution operator of the phonon-only Hamiltonian and of the interaction operator written in the Heisenberg representation with respect to the phonon-only Hamiltonian. In the harmonic case, this corresponds to the creation and annihilation operators for the different phonon normal modes becoming time dependent with a phase factor that is $\exp[\pm i\omega_\nu t]$ for the creation and annihilation operator. If we include the anharmonic phonon potential terms into the phonon-only Hamiltonian, then the Heisenberg representation (with respect to the phonon-only Hamiltonian) of the creation and annihilation operators is more complicated, because the anharmonic terms do not have simple commutation relations with the creation and annihilation operators. Analyzing this exactly becomes cumbersome. In condensed matter physics, one often invokes a so-called quasiharmonic approximation to treat such complexities approximately. The quasiharmonic approximation takes the anharmonic system and replaces it with an equivalent harmonic one, where the phonon frequencies are chosen to vary with the phonon occupancies in the same way that the phonon frequencies are shifted due to the anharmonic terms. Hence, we use the traditional modification

of the creation and annihilation operators by a time-dependent phase factor, $\exp[\pm i(\omega_\nu + \Delta\omega_\nu(n_\nu, \{n_{\nu'}\}))t]$, that incorporates the anharmonic shifts. We use this approach in approximately treating the anharmonic effects on the effective spin-spin interactions. The corrections to these expressions must arise from additional commutator effects and should be smaller than the energy shifts that we include. Once this is done, the derivation of the spin-spin interactions is unchanged from the harmonic case, with the exception of using the shifted frequencies.

Note that the average occupation number of each phonon mode can be shown to be $\bar{n}_\nu = [\exp(\hbar\omega_\nu/k_B T) - 1]^{-1}$ when the ion chain is in thermal equilibrium at a temperature T. Then, instead of calculating the anharmonic frequency shifts (and thus the anharmonic spin-spin interactions) in terms of the occupation numbers, one can write the average occupation numbers as a function of the temperature, and thus $\Delta\omega_\nu = \Delta\omega_\nu(T)$. Specifically, there are two temperature limits relevant to current experimental efforts. The first regime is the Doppler cooling limit for all modes, where the temperature reached is of the order of a few hundred microkelvins. The second temperature regime is Doppler cooling plus sideband cooling on the transverse modes. For our purposes, the sideband cooling will lead to effectively zero occupation of the transverse modes, but the longitudinal modes remain at the Doppler limit temperature. Our assumption for the cooling is that the Doppler cooling, which is applied to all of the modes, occurs from a broad atomic resonance that is much broader than the bandwidth of the phonons, so that all of the phonons are cooled to a temperature that is proportional to the width of the atomic resonance. The sideband cooling works with a separate narrow atomic transition which allows one to remove all of the phonons in a particular phonon band (like the transverse modes). Given a fixed temperature for the different phonon modes, one can then determine their occupation number from simple Bose statistics, as described above.

III. NUMERICAL RESULTS

In this section, we present numerical examples to illustrate how anharmonic couplings affect the frequencies and spin-spin interactions between ions in the linear Paul trap. The parameters we use reflect typical parameters used in current experimental efforts. The longitudinal trapping frequency is $\omega_z = 2\pi \times 500$ kHz, and the transverse trapping frequencies are given by $\beta_x = \beta_y = 10$. Furthermore, we consider a trap with 24 ions arranged in it, which, for the above parameters, is the maximum number of ions without a zigzag transition (unstable modes); i.e., the ion equilibrium positions lie in a linear chain. The trapped ions are Yb^{171+}. Note that for these parameters, the Doppler cooling limit is set by the transverse center-of-mass frequency and is of the order of $k_B T \approx \hbar\omega_{\text{c.m.}}$. This implies the longitudinal modes should have of the order of 1 to 10 quanta excited at the Doppler cooling limit.

A. Frequency shifts

First, we examine the effects of the anharmonicities on the frequencies of the modes. Figure 1 shows the anharmonic shifts of the longitudinal and transverse frequencies both for
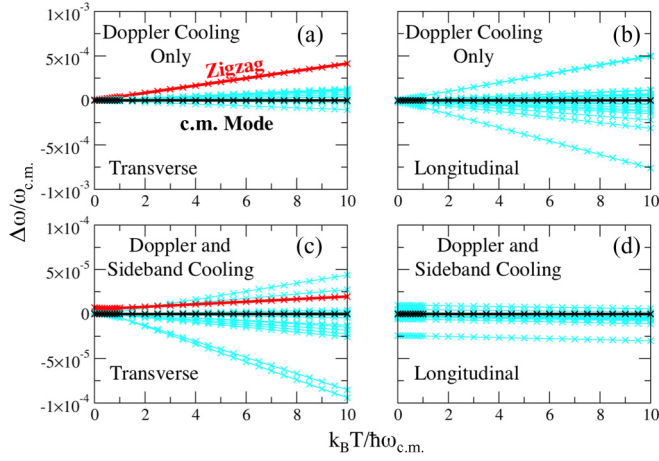
FIG. 1. (Color online) Anharmonic frequency shifts as a function of the temperature of the phonon modes measured relative to the transverse center-of-mass phonon frequency $\omega_{\rm c.m.}$. The center-of-mass mode is shown in black in all panels, while the transverse zigzag mode is shown in dark gray (red) in (a) and (c). All other modes are shown in light gray (cyan). (a) Frequency shifts of transverse modes in the Doppler cooling limit, where both transverse and longitudinal phonons are at temperature T. (b) Shifts of the longitudinal modes in the Doppler cooling limit. (c) Shifts of transverse modes with Doppler and sideband cooling (zero transverse phonon occupation, so transverse phonons are in the ground state, while longitudinal ones are at temperature T). (d) Shifts of longitudinal modes with Doppler and sideband cooling (zero transverse phonon occupation).
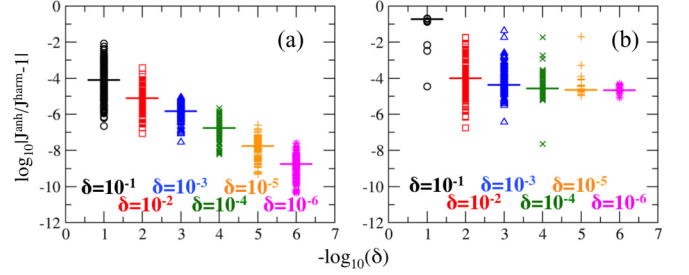

FIG. 2. (Color online) (a) Proportional shifts in spin-spin interactions for detunings above the center-of-mass mode. (b) The same for detunings above the fifth lowest transverse frequency mode. Both plots are shown for $\delta = 10^{-1}$, $\delta = 10^{-2}$, $\delta = 10^{-3}$, $\delta = 10^{-4}$, $\delta = 10^{-5}$, and $\delta = 10^{-6}$. Symbols show the shifts for all ($24 \times 23/2 = 276$) spin-spin interactions J_{ij}. Solid horizontal lines show the corresponding average shift.

Doppler cooling only and for Doppler cooling with sideband cooling of the transverse modes.

A few trends are immediately noticeable. First, the shifts remain smaller than the order of $10^{-4}\omega_{\rm c.m.}$ for the case of Doppler cooling only [Figs. 1(a) and 1(b)] and smaller than the order of $10^{-5}\omega_{\rm c.m.}$ for the case with sideband cooling also [Figs. 1(c) and 1(d)]. This suggests not only that the anharmonic frequency shifts are relatively small, but also that sideband cooling can suppress these shifts another order of magnitude. Furthermore, it is worth noting that, as anticipated analytically, the shifts for both the transverse and the longitudinal center-of-mass modes are 0 (black lines in Fig. 1). In an experiment with the center-of-mass frequency of the order of a megahertz, the anharmonic shift would be below the order of 100 Hz for Doppler cooling and below 10 Hz for Doppler-plus-sideband cooling. We expect effects of the order of 100 Hz to be experimentally observable, but smaller shifts will be difficult to see and are unlikely to affect other aspects of the experiments. In addition, other effects on the experiment are likely to be more important than these intrinsic anharmonic frequency shifts, when the shifts become so small.

The frequency shift curves are most nearly linear in temperature. This may be surprising considering that the expression for ΔE has a quadratic dependency on the occupation numbers of different modes (cf. Appendix C). However, when we take $\Delta E(n_\nu + 1, \{n_{\nu'}\}) - \Delta E(n_\nu, \{n_{\nu'}\})$, the quadratic dependencies cancel out, and since n_ν is roughly linear with temperature except at extremely low temperatures (in this case, temperatures below the Doppler limit), we find that the frequency shifts are linear with temperature.

Next, we consider the shifts in the effective static spin-spin interactions. Particularly, we discuss how the spin-spin interactions are affected when $\mu = \omega_\nu(1 + \delta)$, for which we say that the spin-spin interactions are detuned by δ above mode ν. Figure 2 plots the proportional change in the spin-spin interactions between the harmonic and the anharmonic Hamiltonians for Doppler cooling only with a temperature that satisfies $k_B T = 10\hbar\omega_z \approx \hbar\omega_{\rm c.m.}$. Figure 2(a) shows the shifts in the spin-spin interactions for detunings above the transverse center-of-mass mode, while Fig. 2(b) has detunings above the fifth lowest transverse frequency. We choose a wide range of detunings for completeness, even if some may be difficult to achieve in an actual experiment.

Clearly, Fig. 2(a) exhibits negligible shifts, especially for detunings smaller than $\delta = 10^{-2}$. For the $\delta = 10^{-1}$ detuning (black curve), the spin interactions are shifted by as much as 1%, although the average is more toward the order of 0.01%. Furthermore, as the detuning decreases by an order of magnitude, so do the shifts. In this vein, the smallest detuning of $\delta = 10^{-6}$ (magenta curve) shifts the spin-spin interactions by a factor of approximately 10^{-9}. These shifts are obviously negligible.

On the other hand, Fig. 2(b), which shows detuning above the fifth lowest frequency mode, exhibits quite different behavior. First, the shifts are on average about 10% for the largest detuning (black curve). Furthermore, for detunings as small as 10^{-5}, there are still shifts by a factor of 1%, although the average shift is more toward 0.01% for these smaller detunings. Then, in general, the anharmonic effects on the spin-spin interactions are not negligible for this case, even for the small detunings.

This phenomenon can be attributed to the fact that $\Delta\omega_{\rm c.m.} = 0$. Since the shift in the center-of-mass frequency is 0, the changes in $J_{i,j}$ that one might expect to see due to the $(\mu^2 - \omega_{\rm c.m.}^2)^{-1}$ term are largely suppressed. However, due to nonzero shifts in frequency for other modes, detuning above other modes makes the spin-spin interactions more sensitive to anharmonic effects.

Figure 3 shows how the spin-spin interactions between the first ion and every other ion shift as a function of temperature
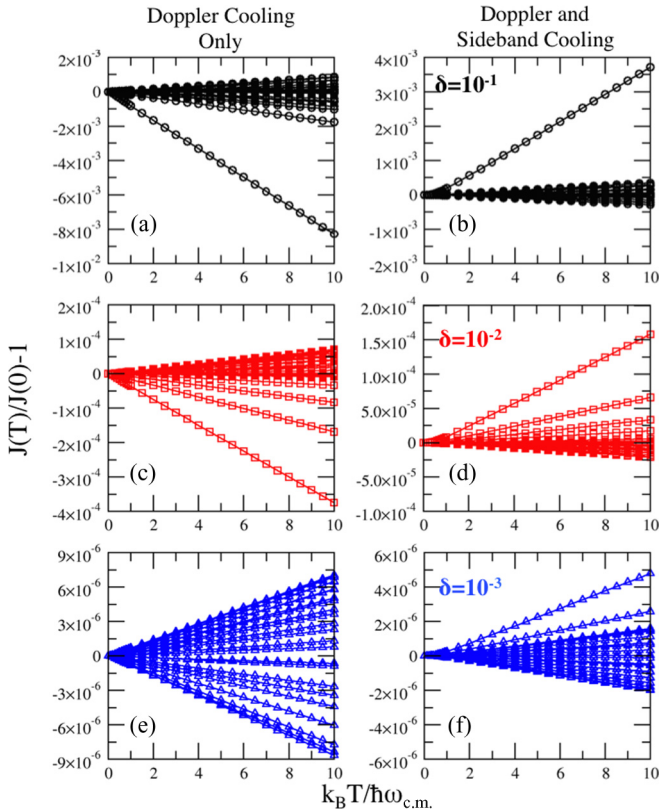
FIG. 3. (Color online) Dependence of the spin-spin interactions detuned above the center-of-mass mode as a function of the system's temperature. Left: Doppler cooling only. Right: Doppler plus sideband cooling. Spin-spin interactions plotted are J_{1j}, that is, spin interactions between the leftmost ion in the chain and every other ion, and we use three detunings, corresponding to the three colors. The most significant trend in this plot is that the shifts are nearly linear as a function of temperature. Furthermore, in (a) and (b), and even in (c) and (d), there are clear outliers that shift much more than the other lines. As expected, these lines plot spin interactions between ions on either side of the chain; the shifts are proportionally large because the spin-spin interactions between distant sites are quite small to begin with, hence the effects of these shifts on the dynamics of the system, even though they appear to be large, are likely to be rather small.

for detunings above the center of mass. The spin-spin interactions appear roughly linear as a function of temperature. Furthermore, particularly for the larger detunings, there are some outliers that shift significantly more than the others. These shifts are for the interactions between the first ion and the ion that is farthest away. Since these interactions themselves are small for larger detunings and far distances, even small changes in the spin interactions will change the interaction between these sites by a significant amount. In fact, even for the 10^{-1} detuning, many of the interactions change by no more than a factor of 10^{-7}.

Finally, we found an interesting trend in the harmonic spin-spin interactions that warrants further discussion. Figure 4 shows the harmonic spin-spin couplings $J_{i,j}$'s as a function of the distance between the interacting spins (all $24 \times 23/2 = 276$ spin-spin couplings are plotted). As a whole, the graph is in fact fairly typical: the smallest detunings produce the largest
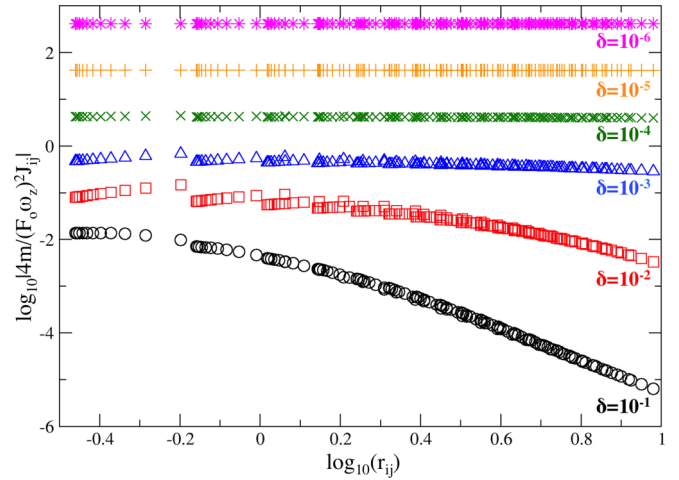

FIG. 4. (Color online) Harmonic spin-spin interactions as a function of the distance between interacting spins. Note that for intermediate detuning, $\delta = 10^{-2}$ [(red) square] and $\delta = 10^{-3}$ [(blue) triangle] curves, and for small separations between spins, there can be increasing spin interactions for increasing separation between the ions. This suggests that ions towards either end of the chain interact more strongly with their neighbors than those in the middle of the chain do, a surprising result since ions in the middle of the chain are closer together. For larger distances, spin-spin couplings become approximate power laws, as expected.

spin interactions (which are approximately constant), while the largest detunings cause smaller spin-spin interactions that fall off like $J = r^{-3}$. However, if one looks closely at the curves corresponding to intermediate detunings $\delta = 10^{-3}$ and $\delta = 10^{-2}$ [(blue) triangle and (red) square curves, respectively], then one notices local regions at small distances (less than the characteristic length) for which the spin interactions *increase* as the distance between the interacting ions increases. Essentially, since nearest-neighbor ions on the inside of the chain are compressed more closely together than neighbors on the outer edges of the chain, this suggests that ions toward the outside of the chain interact more strongly with their neighbors than the inner ions do with their neighbors. This effect is also readily seen for smaller detunings, although the scale of Fig. 4 does not easily show this. Such spin-spin couplings could potentially allow for interesting types of spin models to be examined, since the couplings change character—initially growing with distance and then decaying, and they also show that it is not always true that the spin-spin couplings can be described by a simple power-law behavior, as is often assumed. This behavior is due to the fact that the phonon modes with frequencies close to the center-of-mass mode (such as the tilt mode) have larger phonon displacements for the ions farthest from the center than phonon modes farther from the center-of-mass phonon frequency, hence the ions farther away make a larger contribution to the spin-spin interaction coming from the tilt mode. As the detuning is increased from 0, the tilt mode and other phonon modes with similar properties enter the summation that determines the spin-spin interactions with a higher weight than phonon modes that emphasize motion toward the center of the chain. This result gives rise to the anomalous increase in the spin-spin

interactions for nearest neighbors and for second nearest neighbors at intermediate detunings. When one is detuned sufficiently far from the center-of-mass mode, then all modes contribute equally, and the spin-spin couplings decay like the inverse third power of the distance between the ions. Hence, once the detuning is large enough, this anomalous behavior disappears.

IV. CONCLUSION AND DISCUSSION

In this work, we have treated the anharmonic effects in the linear Paul trap due to the Coulomb interaction to fourth order in order to consider the effects of anharmonic couplings on the normal-mode frequencies and spin-spin interactions between trapped ions. We find that the frequency shifts are small (of the order of $10^{-4}\omega_{\text{c.m.}}$) when only Doppler cooling is utilized and another order of magnitude smaller when sideband cooling is also implemented. Furthermore, we find that spin-spin interactions that are detuned above the center-of-mass mode change by no more than a factor of 10^{-4} except at the largest detuning considered. This lack of significant change is a consequence of the fact that $\Delta\omega_{\text{c.m.}} = 0$. However, for spin interactions detuned near other modes, the anharmonic couplings can have an appreciable effect, as large as 10% for the largest detuning considered and as large as 1% for the smaller detunings. Finally, we find that the spins toward the ends of the ion chain counterintuitively interact more strongly with their neighbors than do the spins on the inside of the chain for a wide range of detunings to the blue of the transverse center-of-mass mode. The mechanism behind this phenomenon follows by analyzing the contributions of the different phonon eigenmodes to the spin-spin couplings. The modes closest to the center-of-mass mode have the largest relative phonon displacements for ions farthest from the center of the trap, compared to those that have phonon frequencies farther from the center-of-mass frequency, where the ion motion of the normal modes is dominated by ions closer to the center of the trap, and this results in the anomalous behavior.

ACKNOWLEDGMENTS

APPENDIX A: DERIVATION OF THE ANHARMONIC COUPLING HAMILTONIAN

In order to generate the Hamiltonian given by Eq. (2), first we expand the potential to fourth order about the equilibrium positions of the ions, and then we transform this result from the ion-position basis to the phonon-mode basis. Let $\mathcal{H}_0$ denote the harmonic Hamiltonian for the system. Then

$$
\mathcal{H} = \mathcal{H}_0 + \frac{1}{6} \sum_{\substack{\alpha,\beta,\gamma \\ = x,y,z}} \sum_{i,j,k=1}^{N} \frac{\partial^3 V}{\partial x_{\alpha i} \partial x_{\beta j} \partial x_{\gamma k}} \bigg|_0 \epsilon_{\alpha i}\epsilon_{\beta j}\epsilon_{\gamma k}
$$
$$
+ \frac{1}{24} \sum_{\substack{\alpha,\beta,\gamma,\delta \\ = x,y,z}} \sum_{i,j,k,l=1}^{N} \frac{\partial^4 V}{\partial x_{\alpha i} \partial x_{\beta j} \partial x_{\gamma k} \partial x_{\delta l}} \bigg|_0
$$
$$
\times \epsilon_{\alpha i}\epsilon_{\beta j}\epsilon_{\gamma k}\epsilon_{\delta l}, \tag{A1}
$$

where $\epsilon_{\alpha i}$ is given by $\epsilon_{\alpha i} = x_{\alpha i} - x_{\alpha i}^0$ for equilibrium positions $x_{\alpha i}^0$ and where the partial derivatives are evaluated at the equilibrium positions.

Now define

$$
\tilde{B}_{\alpha i,\beta j,\gamma k} = \frac{\partial^3 V}{\partial x_{\alpha i} \partial x_{\beta j} \partial x_{\gamma k}} \bigg|_0 \tag{A2}
$$

and

$$
\tilde{C}_{\alpha i,\beta j,\gamma k,\delta l} = \frac{\partial^4 V}{\partial x_{\alpha i} \partial x_{\beta j} \partial x_{\gamma k} \partial x_{\delta l}} \bigg|_0. \tag{A3}
$$

These tensors can of course be solved for by taking the third and fourth derivatives of the potential [given by Eq. (1)] and then evaluating them at the equilibrium positions of the ions (which is what the subscript 0 indicates). However, the calculations themselves are quite tedious, so the lengthy algebra is omitted. The final results for $\tilde{B}$ and $\tilde{C}$ are shown in Appendix B.

Now we must change to the phonon-mode basis. In the phonon-mode basis, the harmonic Hamiltonian is given in terms of the creation and annihilation operators, and the displacement from equilibrium $\epsilon_{\alpha i}$ is replaced by the phonon displacement operator X_ν, which must be summed over all phonon modes and weighted by the normal-mode eigenvectors to yield the total displacement. The Hamiltonian becomes

$$
\mathcal{H} = \mathcal{H}_0^{\text{phon}} + \frac{1}{6} \sum_{\{\alpha,\beta,\gamma = x,y,z\}} \sum_{\{i,j,k=1\}}^{N} \sum_{\{\nu,\nu',\nu''=1\}}^{3N} b_i^{\alpha\nu} b_j^{\beta\nu'} b_k^{\gamma\nu''} \tilde{B}_{\alpha i,\beta j,\gamma k} X_\nu X_{\nu'} X_{\nu''}
$$
$$
+ \frac{1}{24} \sum_{\{\alpha,\beta,\gamma,\delta = x,y,z\}} \sum_{\{i,j,k,l=1\}}^{N} \sum_{\{\nu,\nu',\nu'',\nu'''=1\}}^{3N} b_i^{\alpha\nu} b_j^{\beta\nu'} b_k^{\gamma\nu''} b_l^{\delta\nu'''} \tilde{C}_{\alpha i,\beta j,\gamma k,\delta l} X_\nu X_{\nu'} X_{\nu''} X_{\nu'''}, \tag{A4}
$$

where the symbol $b_i^{\alpha\nu}$ denotes the eigenvector of the harmonic phonon Hamiltonian for the νth mode, showing the displacement of the ith ion in the αth direction [14]. Define the ladder operators

$$\hat{a}_\nu = \sqrt{\frac{1}{2\varepsilon_\nu}}\left(\frac{\omega_\nu}{\omega_z}X_\nu + iP_\nu\right),$$

$$\hat{a}_\nu^\dagger = \sqrt{\frac{1}{2\varepsilon_\nu}}\left(\frac{\omega_\nu}{\omega_z}X_\nu - iP_\nu\right),$$

(A5)

which satisfy the canonical commutation relations $[a_\nu, a_{\nu'}^\dagger] = \delta_{\nu\nu'}$. Then, by expressing the Hamiltonian in terms of the phonon creation and annihilation operators, we obtain [14]

$$\mathcal{H} = \sum_{\nu=1}^{3N}\varepsilon_\nu\left(\hat{a}_\nu^\dagger\hat{a}_\nu + \frac{1}{2}\right) + \sum_{\nu,\nu',\nu''=1}^{3N}B_{\nu,\nu',\nu''}(\hat{a}_\nu + \hat{a}_\nu^\dagger)(\hat{a}_{\nu'} + \hat{a}_{\nu'}^\dagger)(\hat{a}_{\nu''} + \hat{a}_{\nu''}^\dagger)$$

$$+ \sum_{\nu,\nu',\nu'',\nu'''=1}^{3N}C_{\nu,\nu',\nu'',\nu'''}(\hat{a}_\nu + \hat{a}_\nu^\dagger)(\hat{a}_{\nu'} + \hat{a}_{\nu'}^\dagger)(\hat{a}_{\nu''} + \hat{a}_{\nu''}^\dagger)(\hat{a}_{\nu'''} + \hat{a}_{\nu'''}^\dagger),$$

(A6)

where

$$B_{\nu,\nu',\nu''} = \frac{1}{6}\left(\frac{\hbar}{2ml_0^2}\right)^{3/2}(\omega_\nu\omega_{\nu'}\omega_{\nu''})^{-1/2}\sum_{\{i,j,k=1\}}^{3N}\sum_{\{\alpha,\beta,\gamma=x,y,z\}}\tilde{B}_{\alpha i,\beta j,\gamma k}b_i^{\alpha\nu}b_j^{\beta\nu'}b_k^{\gamma\nu''}$$

(A7)

and

$$C_{\nu,\nu',\nu'',\nu'''} = \frac{1}{24}\left(\frac{\hbar}{2ml_0^2}\right)^2(\omega_\nu\omega_{\nu'}\omega_{\nu''}\omega_{\nu'''})^{-1/2}\sum_{\{i,j,k,l=1\}}^{3N}\sum_{\{\alpha,\beta,\gamma,\delta=x,y,z\}}\tilde{C}_{\alpha i,\beta j,\gamma k,\delta l}b_i^{\alpha\nu}b_j^{\beta\nu'}b_k^{\gamma\nu''}b_l^{\delta\nu'''}.$$

(A8)

Note that B and C are simply the coefficients of the third- and fourth-order potential terms ($\tilde{B}$ and $\tilde{C}$ are in the ion-position basis) written in the phonon basis with some constants absorbed.

APPENDIX B: EXPRESSIONS FOR $\tilde{B}$ AND $\tilde{C}$

We now evaluate the exact expressions for the cubic and quartic phonon-mode coupling tensors in terms of the equilibrium positions, as follows:

$$\alpha = \{x,y\} : \tilde{B}_{\alpha i,\alpha j,zk} = \begin{cases} -3\sum_{\substack{h=1\\h\neq i}}^{N}\frac{\mathrm{sgn}(h-i)}{\left|x_{zh}^0 - x_{zi}^0\right|^4}, & i=j=k; \\ 3\frac{\mathrm{sgn}(j-i)}{|x_{zj}^0-x_{zi}^0|^4}, & \text{two indices are } i, \text{ the other is } j; \\ 0, & i\neq j, j\neq k, k\neq i. \end{cases}$$

$$\tilde{B}_{zi,zj,zk} = \begin{cases} 6\sum_{\substack{h=1\\h\neq i}}^{N}\frac{\mathrm{sgn}(h-i)}{\left|x_{zh}^0 - x_{zi}^0\right|^4}, & i=j=k; \\ -6\frac{\mathrm{sgn}(j-i)}{\left|x_{zj}^0-x_{zi}^0\right|^4}, & \text{two indices are } i, \text{ the other is } j; \\ 0, & i\neq j, j\neq k, k\neq i. \end{cases}$$

$$\alpha = \{x,y\} : \tilde{C}_{\alpha i,\alpha j,\alpha k,\alpha l} = \begin{cases} \sum_{\substack{h=1\\h\neq i}}^{N}\frac{9}{\left|x_{zh}^0-x_{zi}^0\right|^5}, & i=j=k=l; \\ \frac{-9}{\left|x_{zi}^0-x_{zj}^0\right|^5}, & \text{three indices are } i, \text{ the other is } j; \\ \frac{9}{\left|x_{zi}^0-x_{zj}^0\right|^5}, & \text{two indices are } i, \text{ the other two are } j; \\ 0 & \text{otherwise.} \end{cases}$$

$$\alpha,\beta = \{x,y\}; \alpha\neq\beta : \tilde{C}_{\alpha i,\alpha j,\beta k,\beta l} = \begin{cases} \sum_{\substack{h=1\\h\neq i}}^{N}\frac{3}{\left|x_{zh}^0-x_{zi}^0\right|^5}, & i=j=k=l; \\ \frac{-3}{\left|x_{zi}^0-x_{zj}^0\right|^5}, & \text{three indices are } i, \text{ the other is } j; \\ \frac{3}{\left|x_{zi}^0-x_{zj}^0\right|^5}, & \text{two indices are } i, \text{ the other two are } j; \\ 0 & \text{otherwise.} \end{cases}$$

$$\alpha = \{x,y\} : \tilde{C}_{\alpha i,\alpha j,zk,zl} = \begin{cases} \sum_{\substack{h=1 \\ h \neq i}}^{N} \frac{-12}{\left|x_{zh}^0 - x_{zi}^0\right|^5}, & i = j = k = l; \\ \frac{12}{\left|x_{zi}^0 - x_{zj}^0\right|^5}, & \text{three indices are } i, \text{ the other is } j; \\ \frac{-12}{\left|x_{zi}^0 - x_{zj}^0\right|^5}, & \text{two indices are } i, \text{ the other two are j;} \\ 0 & \text{otherwise.} \end{cases}$$

$$\tilde{C}_{zi,zj,zk,zl} = \begin{cases} \sum_{\substack{h=1 \\ h \neq i}}^{N} \frac{24}{\left|x_{zh}^0 - x_{zi}^0\right|^5}, & i = j = k = l; \\ \frac{-24}{\left|x_{zi}^0 - x_{zj}^0\right|^5}, & \text{three indices are } i, \text{ the other is } j; \\ \frac{24}{\left|x_{zi}^0 - x_{zj}^0\right|^5}, & \text{two indices are } i; \text{ the other two are } j; \\ 0 & \text{otherwise.} \end{cases}$$

APPENDIX C: DERIVATION OF ANHARMONIC ENERGY SHIFTS VIA NONDEGENERATE PERTURBATION THEORY

To solve for the energy shifts, we consider the first- and second-order Rayleigh-Schrödinger corrections for the quartic and cubic perturbations, respectively. The anharmonic energy shifts are then given by the following:

$$\Delta E(\{n_\nu\}) = {}_0\langle\{n_\nu\}|V^{(4)}|\{n_\nu\}\rangle_0 + \sum_{\{m_\nu\} \neq \{n_\nu\}} \frac{|{}_0\langle\{m_\nu\}|V^{(3)}|\{n_\nu\}\rangle_0|^2}{E_n^0 - E_m^0}. \tag{C1}$$

Recall that the first-order correction for the third-order potential term is 0 since there are an odd number of creation and annihilation operators. Furthermore, recall that we ignore the second-order correction for the fourth-order potential term.

Keeping in mind that $E_n^0 = \sum_{\nu=1}^{3N} \varepsilon_\nu(n_\nu + \frac{1}{2})$ and that

$$V^{(3)} = \sum_{\nu,\nu',\nu''=1}^{3N} B_{\nu,\nu',\nu''}(\hat{a}_\nu^\dagger + \hat{a}_\nu)(\hat{a}_{\nu'}^\dagger + \hat{a}_{\nu'})(\hat{a}_{\nu''}^\dagger + \hat{a}_{\nu''}), \tag{C2}$$

$$V^{(4)} = \sum_{\nu,\nu',\nu'',\nu'''=1}^{3N} C_{\nu,\nu',\nu'',\nu'''}(\hat{a}_\nu^\dagger + \hat{a}_\nu)(\hat{a}_{\nu'}^\dagger + \hat{a}_{\nu'})(\hat{a}_{\nu''}^\dagger + \hat{a}_{\nu''})(\hat{a}_{\nu'''}^\dagger + \hat{a}_{\nu'''}), \tag{C3}$$

one can directly solve for the anharmonic energy shifts. After some tedious algebra, the final expression for the anharmonic energy shifts becomes

$$\Delta E(\{n_\nu\}) = 3 \sum_{\nu=1}^{3N} \left[(2n_\nu^2 + 2n_\nu + 1)C_{\nu,\nu,\nu,\nu} + 2(2n_\nu + 1)\sum_{\nu'\neq\nu}^{3N}(2n_{\nu'} + 1)C_{\nu,\nu,\nu',\nu'} \right]$$

$$+ \left(\frac{\omega_z^2 l_0^2 m}{\hbar}\right) \left[-\sum_{\nu=1}^{3N} B_{\nu,\nu,\nu}^2 \frac{30n_\nu^2 + 30n_\nu + 11}{\omega_\nu} - 18\sum_{\nu=1}^{3N}\sum_{\nu'\neq\nu}^{3N} B_{\nu',\nu',\nu}B_{\nu,\nu,\nu} \frac{(2n_{\nu'} + 1)(2n_\nu + 1)}{\omega_\nu} \right.$$

$$+ 9\sum_{\nu=1}^{3N}\sum_{\nu'\neq\nu}^{3N} B_{\nu',\nu',\nu}^2 \left(\frac{-4\omega_{\nu'}(2n_{\nu'} + 1)(2n_\nu + 1)}{4\omega_{\nu'}^2 - \omega_\nu^2} + \frac{2(n_{\nu'}^2 + n_{\nu'} + 1)}{4\omega_{\nu'}^2 - \omega_\nu^2} - \frac{(2n_{\nu'} + 1)^2}{\omega_\nu}\right) - 18\sum_{\nu=1}^{3N}\sum_{\nu'\neq\nu}^{3N}\sum_{\substack{\nu''\neq\nu \\ \nu''\neq\nu'}}^{3N} B_{\nu',\nu',\nu}$$

$$\times B_{\nu'',\nu'',\nu} \frac{(2n_{\nu'} + 1)(2n_{\nu''} + 1)}{\omega_\nu} + 36\sum_{\nu=1}^{3N}\sum_{\nu'\neq\nu}^{3N}\sum_{\substack{\nu''\neq\nu \\ \nu''\neq\nu'}}^{3N} B_{\nu',\nu',\nu''}^2 \left(-\frac{(\omega_\nu + \omega_{\nu'})(1 + n_\nu + n_{\nu'})(2n_{\nu''} + 1)}{(\omega_\nu + \omega_{\nu'})^2 - \omega_{\nu''}^2}\right.$$

$$\left.\left. + \frac{\omega_{\nu''}(1 + n_\nu + n_{\nu'} + 2n_\nu n_{\nu'})}{(\omega_\nu + \omega_{\nu'})^2 - \omega_{\nu''}^2} + \frac{(\omega_\nu - \omega_{\nu'})(n_\nu - n_{\nu'})(2n_{\nu''} + 1)}{(\omega_\nu - \omega_{\nu'})^2 - \omega_{\nu''}^2} + \frac{\omega_{\nu''}(n_\nu + n_{\nu'} + 2n_\nu n_{\nu'})}{(\omega_\nu - \omega_{\nu'})^2 - \omega_{\nu''}^2}\right)\right]. \tag{C4}$$

This formula is used to evaluate the anharmonic shifts in the phonon frequencies throughout this paper. Note that these formulas are at most quadratic in the phonon occupation numbers and become linear when differences are taken with neighboring occupancies. Hence, we only need the average phonon number in each mode for the thermal distributions to determine the temperature-dependent shifts.

[1] R. P. Feynman, Int. J. Theor. Phys. **21**, 467 (1982).

[2] A. Friedenauer, H. Schmitz, J. T. Glueckert, D. Porras, and T. Schaetz, Nat. Phys. **4**, 757 (2008).

[3] K. Kim, M.-S. Chang, R. Islam, S. Korenblit, L.-M. Duan, and C. Monroe, Phys. Rev. Lett. **103**, 120502 (2009).

[4] K. Kim, M.-S. Chang, S. Korenblit, R. Islam, E. E. Edwards, J. K. Freericks, G.-D. Lin, L.-M. Duan, and C. Monroe, Nature **465**, 590 (2010).

[5] E. E. Edwards, S. Korenblit, K. Kim, R. Islam, M.-S. Chang, J. K. Freericks, G.-D. Lin, L.-M. Duan, and C. Monroe, Phys. Rev. B **82**, 060412(R) (2010).

[6] R. Islam, E. E. Edwards, K. Kim, S. Korenblit, C. Noh, H. Carmichael, G.-D. Lin, L.-M. Duan, C.-C. J. Wang, J. K. Freericks, and C. Monroe, Nature Commun. **2**, 377 (2011).

[7] J. W. Britton, B. C. Sawyer, A. C. Keith, C.-C. J. Wang, J. K. Freericks, M. J. Biercuk, H. Uys, and J. J. Bollinger, Nature **484**, 489 (2012).

[8] B. C. Sawyer, J. W. Britton, A. C. Keith, C.-C. Joseph Wang, J. K. Freericks, H. Uys, M. J. Biercuk, and J. J. Bollinger, Phys. Rev. Lett. **108**, 213003 (2012).

[9] B. P. Lanyon, C. Hempel, D. Nigg, M. Müller, R. Gerritsma, F. Zähringer, P. Schindler, J. T. Barreiro, M. Rambach, G. Kirchmair, M. Hennrich, P. Zoller, R. Blatt, and C. F. Roos, Science **334**, 57 (2011).

[10] R. Islam, C. Senko, W. C. Campbell, S. Korenblit, J. Smith, A. Lee, E. E. Edwards, C.-C. J. Wang, J. K. Freericks, and C. Monroe, Science **340**, 583 (2013).

[11] P. Richerme, Z.-X. Gong, A. Lee, C. Senko, J. Smith, M. Foss-Feig, S. Michalakis, A. V. Gorshkov, and C. Monroe, Nature **511**, 198 (2014).

[12] P. Jurcevic, B. P. Lanyon, P. Hauke, C. Hempel, P. Zoller, R. Blatt, and C. F. Roos, Nature **511**, 202 (2014).

[13] C. Senko, J. Smith, P. Richerme, A. Lee, W. C. Campbell, and C. Monroe, Science **345**, 430 (2014).

[14] C. Marquet, F. Schmidt-Kaler, and D. F. V. James, Appl. Phys. B **76**, 199 (2003).

[15] C. F. Roos, T. Monz, K. Kim, M. Riebe, H. Häffner, D. F. V. James, and R. Blatt, Phys. Rev. A **77**, 040302(R) (2008).

[16] J. P. Home, D. Hanneke, J. D. Jost, D. Leibfried, and D. J. Wineland, New J. Phys. **13**, 073026 (2011).

[17] Z.-X. Gong, G.-D. Lin, and L.-M. Duan, Phys. Rev. Lett. **105**, 265703 (2010).

[18] D. J. Wineland and H. G. Dehmelt, J. Appl. Phys. **46**, 919 (1975).

[19] T. M. Oneil and D. H. E. Dubin, Phys. Plasmas **5**, 2163 (1998).

[20] D. Porras and J. I. Cirac, Phys. Rev. Lett. **92**, 207901 (2004).

[21] S.-L. Zhu, C. Monroe, and L.-M. Duan, Phys. Rev. Lett. **97**, 050505 (2006).

[22] C.-C. Joseph Wang and J. K. Freericks, Phys. Rev. A **86**, 032329 (2012).